

NASA TECHNICAL NOTE



NASA TN D-4423

C.1

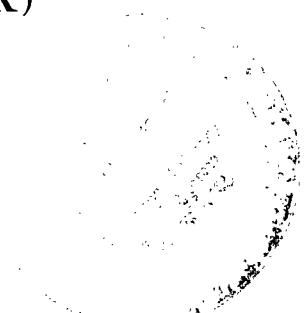
NASA TN D-4423



LOAN COPY: RETURN TO
AFWL (WLIL-2)
KIRTLAND AFB, N MEX

CHANGE IN INDUCER NET POSITIVE
SUCTION HEAD REQUIREMENT WITH
FLOW COEFFICIENT IN LOW TEMPERATURE
HYDROGEN (27.9° TO 36.6° R)

by Phillip R. Meng
Lewis Research Center
Cleveland, Ohio





CHANGE IN INDUCER NET POSITIVE SUCTION HEAD REQUIREMENT
WITH FLOW COEFFICIENT IN LOW TEMPERATURE
HYDROGEN (27.9⁰ TO 36.6⁰ R)

By Phillip R. Meng

Lewis Research Center
Cleveland, Ohio

NATIONAL AERONAUTICS AND SPACE ADMINISTRATION

For sale by the Clearinghouse for Federal Scientific and Technical Information
Springfield, Virginia 22151 - CFSTI price \$3.00

CHANGE IN INDUCER NET POSITIVE SUCTION HEAD REQUIREMENT
WITH FLOW COEFFICIENT IN LOW TEMPERATURE
HYDROGEN (27.9° TO 36.6° R)

by Phillip R. Meng

Lewis Research Center

SUMMARY

An 84° flat plate helical inducer was used to evaluate the thermodynamic effect of cavitation in low temperature liquid hydrogen over a range of flow coefficients. The range of liquid hydrogen temperatures studied was from 27.9° to 36.6° R (15.5° to 20.3° K). The tests were conducted at a rotative speed of 20 000 rpm over a range of flow coefficients from 0.060 to 0.076 (1200 to 1500 gal/min (4.6 to 5.7 m³/min)). For a given head coefficient ratio, the required net positive suction head increased as the fluid inlet temperature was lowered. This decrease in inducer performance was attributed to a decrease in the thermodynamic effect of cavitation at the lower fluid temperatures. For a given temperature the thermodynamic effect of cavitation increased with decreasing flow coefficient. This effect is attributed to changes in blade pressure distribution with flow coefficient.

The measured values of required net positive suction head are in reasonable agreement with those obtained using a semiempirical prediction method.

INTRODUCTION

Space vehicles fueled with liquid hydrogen require large tanks because of the low density of this liquid. A reduction in the required tank volume for a given mission can be obtained by preconditioning the hydrogen fuel to a mixture of liquid and solid hydrogen at 24.9° R (13.8° K) as suggested by several authors (refs. 1 and 2). In such a vehicle feed system, the turbopump may be required to pump liquid hydrogen at temperatures below the normal boiling point of 36.4° R (20.2° K). It has been shown that the cavitation performance of pumps and other flow devices in liquid hydrogen is affected appreciably

ciably by the temperature of the hydrogen (refs. 3 to 5). A cavitating inducer in a rocket engine turbopump is designed to operate with a vapor cavity on the suction surface of the blades. For a given pump speed and inlet pressure, the size of this cavity is dependent on the degree of evaporative cooling that occurs at the liquid-vapor interface as a result of vaporization. Since vaporization involves heat transfer, the amount of cooling realized under given conditions is a function of the physical properties of the fluid, and thus will change with the fluid being pumped as well as with its temperature (refs. 3 to 11). Evaporative cooling causes the vapor pressure of the thin layer of liquid adjacent to the cavity to be reduced by an amount that corresponds to the local temperature reduction; cavity pressure is reduced by a corresponding amount. This reduction in cavity pressure retards the rate of further vapor formation; thereby allowing satisfactory operation of the inducer at lower inlet pressures than would otherwise be possible. The physical properties of liquid hydrogen change appreciably with temperature. Thus the temperature of the hydrogen at the inlet of a pump has a major effect on its cavitation performance. The difference in cavitation performance that occurs between different fluids and over a range of temperature for a given fluid at similar operating conditions are attributed to the thermodynamic effects of cavitation.

It has been shown that a lower value of net positive suction head NPSH was sufficient to maintain a given performance level as the hydrogen temperature was increased from 37.0° to 42.0° R (20.6° to 23.3° K) at a constant speed and flow coefficient (ref. 3). This improvement in cavitation performance was attributed to the increase in the thermodynamic effect of cavitation (fluid property effect) for the higher temperature liquid hydrogen. Conversely, as the hydrogen temperature is decreased, a reduction in the magnitude of the thermodynamic effects of cavitation can be expected. As the temperature of any liquid approaches its triple point temperature, the liquid vapor pressure becomes negligible and the magnitude of thermodynamic effects of cavitation will approach zero. Thus the pump cavitation performance in any liquid near its triple point temperature will approach that obtained in room temperature water, for which the thermodynamic effects are negligible.

A method for predicting the thermodynamic effects of cavitation and thus the cavitation performance of pumps is presented in reference 4. This semiempirical method is based on data obtained from venturi cavitation studies which used several fluids (refs. 6 and 7). Use of this method requires that two appropriate sets of test data be available for the pump of interest. The method was successfully applied in the prediction of the cavitation performance of several research and commercial pumps handling a variety of liquids, including hydrogen, over a range of speeds and temperature levels but for specific values of flow coefficient.

The objective of this investigation was to evaluate the thermodynamic effects of cavitation as determined with an inducer operated in low temperature liquid hydrogen over

a range of flow coefficient. The required NPSH was evaluated for the experimental inducer for a range of flow coefficient from 0.060 to 0.076 (1200 to 1500 gal/min (4.6 to 5.7 m³/min) over a temperature range from 27.9^o to 36.6^o R (15.5^o to 20.3^o K). The results were used in conjunction with an available semiempirical method (ref. 4) to predict the magnitude of the thermodynamic effect of cavitation at various flow coefficients for several hydrogen temperatures. Experimental results were compared with the predicted values of required net positive suction head. The investigation was conducted at the Plum Brook Station of the NASA Lewis Research Center.

APPARATUS AND PROCEDURE

Test Rotor

The test rotor used in this investigation was a three-bladed flat plate helical inducer with a tip helix angle of 84^o. The inducer was similar to the one reported in reference 3 except for a change in the leading edge fairing. The leading edges of the inducer reported herein were faired on the suction surface only, whereas the leading edges of the inducer reported in reference 3 were faired symmetrically to a wedge. A photograph and geometric details of the inducer are shown in figure 1.

Test Facility

This investigation was conducted in the liquid hydrogen pump test facility shown schematically in figure 2. The test inducer was located near the bottom of a 2500-gallon (9.5-m³) stainless-steel vacuum-jacketed tank. A booster rotor, located downstream of the inducer, was used to overcome system losses.

The flow path is through the test inducer and booster rotor to a collector scroll and into a 4.0-inch-diameter (10.2-cm-diam.) line which discharges into a storage dewar. The facility is the same as the one described in detail in reference 3, except for the addition of the vacuum pumps and double seals, which were required for the low temperature tests.

The pressure in the tank ullage was reduced by two large vacuum pumps which were used both to facilitate evaporative cooling of the hydrogen and to control the NPSH during testing. Each pump was rated at 400 cubic feet per minute (11.3 m³/min) at 260^o R (144.4^o K). The 4-inch-diameter (10.2-cm-diam.) line from the research tank to the vacuum pumps was electrically heated in order to maintain the hydrogen gas temperature at or above the rated temperature at the vacuum pump inlets.

Double seals were installed at all line and tank connections to prevent air leakage into the tank during operation at subatmospheric pressure. Helium pressure was applied between the inner and outer seals to further reduce the possibility of air leakage into the hydrogen system.

Test Procedure

The 2500-gallon (9.5-m^3) tank was filled to its maximum capacity with liquid hydrogen at the normal boiling point. Prior to a test, the hydrogen was preconditioned to the desired liquid temperature with the vacuum pumps. The tank was then pressurized to 5 pounds per square inch (34.5 N/cm^2) above the liquid vapor pressure. After the rotor attained the test speed of 20 000 rpm with a constant flow rate, the tank pressure (NPSH) was slowly decreased until the inducer head rise deteriorated because of cavitation. The bulk liquid temperature remained essentially constant during the test duration of from 40 to 70 seconds depending on the flow rate. The noncavitating inducer performance was obtained by operating at a constant speed of 20 000 rpm while maintaining a tank pressure above the liquid vapor pressure (NPSH) of 5 pounds per square inch (34.5 N/cm^2) as the flow rate was varied over the range of interest.

Instrumentation

The location of the instrumentation used in this investigation is shown schematically in figure 3. The measured parameters, number of probes used and the estimated maximum system errors are listed in figure 3.

The liquid vapor pressure was measured at the inducer inlet with a vapor pressure bulb which was charged with hydrogen from the tank. Tank pressure, measured in the ullage space, was used as the reference pressure for the differential pressure transducers. The liquid level above the inducer inlet, measured by a capacitance gage, was added to the reference pressure to correct the differential pressures to inducer-inlet conditions. To obtain the NPSH, the differential pressure measured directly between the vapor bulb pressure and the tank pressure correct to inlet conditions, was converted to head of liquid using the inlet fluid density. An averaged hydrogen temperature at the inducer inlet was obtained from two platinum resistor thermometers. A shielded total pressure probe located at midstream approximately 1 inch (2.54 cm) downstream of the test rotor was used to measure the inducer pressure rise. The shielded probe was set at a 45° angle with the inducer centerline so that the probe would be aligned within the

angle of minimum error during operation over the entire range of flows. Pump flow rate was obtained with a venturi flowmeter which was calibrated in both air and water.

RESULTS AND DISCUSSION

Noncavitating Performance

The noncavitating inducer performance is defined as that which shows no measurable decrease in inducer head rise when the NPSH is either increased or decreased. The noncavitating head coefficient ψ_{NC} for the 84° inducer is plotted as a function of flow coefficient φ for several hydrogen temperatures at NPSH \geq 170 feet (51.8 m) in figure 4. As expected, the hydrogen inlet temperature has no measurable effect on the noncavitating inducer performance. The noncavitating values of head coefficient ψ_{NC} at a given flow coefficient φ are subsequently used to obtain the head coefficient ratio ψ/ψ_{NC} for presenting inducer cavitation data.

Cavitation Performance

The cavitation performance of the inducer for several hydrogen inlet temperatures and flow coefficients is shown in figure 5 where the head coefficient ratio ψ/ψ_{NC} is plotted as a function of NPSH. The data in figure 5 show that for a given head coefficient ratio ψ/ψ_{NC} the required NPSH becomes greater as the temperature is decreased at each value of flow coefficient. As the flow coefficient is decreased, the required value of NPSH is lower for a given head coefficient ratio ψ/ψ_{NC} . The data for a hydrogen temperature of 36.6° R (20.3° K) are not shown for the lower flow coefficients (figs. 5(c) and (d)) because no measurable decrease in head coefficient ratio ψ/ψ_{NC} was noted. At a hydrogen temperature of 34.0° R (18.9° K), the head coefficient ratio ψ/ψ_{NC} exhibits only a slight decrease at values of NPSH above the region where vapor forms in the inlet (figs. 5(c) and (d)). This region is shown as the shaded area on figure 5 and will be discussed later.

The characteristics of this inducer were such that, in some cases, the values of the head coefficient ratio ψ/ψ_{NC} would tend to level off at approximately 0.90 before the head coefficient ratio decreased significantly because of cavitation. An example of this characteristic can be seen in figure 5(a) between values of NPSH from 20 to 45 feet (6.1 to 13.7 m). Because of this inducer characteristic, a head coefficient ratio ψ/ψ_{NC} of 0.70 was used in presenting subsequent cavitation performance data. For this head

coefficient ratio, more consistent comparisons could be made for the various operating conditions.

The vertical dashed lines in figure 5 represent the values of NPSH which correspond to the fluid velocity head $V_a^2/2g$ at the inducer inlet for each value of flow coefficient. When the NPSH is lowered to the value of the inlet velocity head, the local static pressure in the inlet line becomes equal to the fluid vapor pressure. As the pressure is further reduced, the fluid begins to boil in the inlet line and vapor is ingested by the inducer. An increase in through flow velocity resulting from vapor ingestion can cause a shift to a higher flow coefficient as reported in reference 12. Because of this shift in flow coefficient, data taken at values of NPSH less than the inlet velocity head (shaded area of fig. 5) will not be used for subsequent performance comparisons.

In figure 6 the required NPSH for a head coefficient ratio ψ/ψ_{NC} of 0.70 are shown as a function of flow coefficient at the various nominal hydrogen temperature levels. The required NPSH values are shown in figure 6 at the actual measured flow coefficient and are denoted by the same symbol used for the measured hydrogen temperature in figure 5. Additional inducer test data (not shown in fig. 5) are shown as solid symbols in figure 6. The faired curves of figure 6 represent convenient nominal hydrogen temperatures obtained from an arithmetic average of all measured test temperatures. The curves of figure 6 show a significant increase in required NPSH both with increasing flow coefficient and with decreasing hydrogen temperature.

Thermodynamic Effects of Cavitation

The effect of changes in fluid properties on the cavitation process and on the cavitation performance of pumps as described in the INTRODUCTION is discussed in greater detail in references 3 to 6. Venturi cavitation studies (ref. 6) have shown that with flow similarity, that is, a given flow velocity and cavity size, a reduction in cavity pressure allows a corresponding reduction in the inlet pressure requirement (NPSH for a pump). For a pump, it is reasonable to assume that the cavity size or vapor volume is the same at a given head coefficient ratio for all fluids. Experimental performance studies in references 4 and 13 tend to verify this assumption. Thus, in fluids which have appreciable thermodynamic effects, the same vapor volume present in a given pump at a specified performance level would not occur until the NPSH is considerably lower than it would be in fluids which do not exhibit this beneficial effect.

The properties of liquid hydrogen change rapidly with temperature; therefore, a considerable change in the required NPSH can occur with a small change in hydrogen temperature as evidenced by the data of figures 5 and 6. The magnitude of the reduction in vapor pressure due to vaporization Δh_v that can occur with temperature can be esti-

mated from a heat balance study (ref. 3). In this reference, a heat balance between the heat required for vaporization and that drawn from the surrounding liquid is used to show that the cavity pressure reduction Δh_v is closely approximated by

$$\Delta h_v \cong \frac{L}{C_p} \frac{\rho_v}{\rho_l} \left(\frac{dH_{vp}}{dT} \right) \frac{V_v}{V_l} \quad (1)$$

The known properties of liquid hydrogen at various temperatures were used to obtain the values of the vapor to liquid volume ratio V_v/V_l as a function of Δh_v by numerical integration of equation (1). This takes into account changes in properties with temperature during the evaporative cooling process. The calculated reduction in vapor pressure due to vaporization Δh_v is plotted as a function of vapor to liquid volume ratio V_v/V_l for a range of liquid hydrogen temperatures in figure 7. Equation (1) cannot be used directly to predict the required NPSH because in practice the absolute value of V_v/V_l is not known. In a cavitating inducer it may be possible to estimate the vapor volume of the cavity V_v , but the volume of liquid actually involved in the cavitation process V_l cannot be determined. However, from venturi studies (ref. 6) it can be shown that, if a reference value of V_v/V_l is established experimentally by the determination of Δh_v , values of V_v/V_l with respect to the reference value for the conditions of interest can be estimated from the following equation:

$$\frac{V_v}{V_l} = \left(\frac{V_v}{V_l} \right)_{\text{ref}} \left(\frac{\alpha_{\text{ref}}}{\alpha} \right)^{0.5} \left(\frac{\Delta x}{\Delta x_{\text{ref}}} \right)^{0.16} \left(\frac{V_o}{V_{o, \text{ref}}} \right)^{0.85} \quad (2)$$

Since it was assumed that under similar flow conditions the cavity length (vapor volume) at a given head coefficient ratio ψ/ψ_{NC} is essentially a constant, the cavity length term $(\Delta x/\Delta x_{\text{ref}})^{0.16}$ in this equation can be considered as being 1.0. The characteristic velocity V_o is proportional to pump speed N . For this investigation speed was held constant and the term $(V_o/V_{o, \text{ref}})^{0.85}$ also becomes 1.0. Therefore, for a given flow coefficient and value of head coefficient ratio ψ/ψ_{NC} , equation (2) can be stated as

$$\frac{V_v}{V_l} = \left(\frac{V_v}{V_l} \right)_{\text{ref}} \left(\frac{\alpha_{\text{ref}}}{\alpha} \right)^{0.5} \quad (3)$$

A method for predicting pump cavitation performance is presented in reference 4. It is stated that for a constant flow condition and geometrically similar cavities (constant ψ/ψ_{NC}) changes in measured NPSH are equal to the changes in the cavity pressure drop. Thus,

$$NPSH_1 - NPSH_2 = \Delta h_{v_2} - \Delta h_{v_1} \quad (4)$$

The semiempirical relation of reference 4 requires that two experimental test points be available for the pump of interest. These experimental data can be for any combination of liquid, liquid temperature, or rotative speed provided that at least one set of data exhibits a measurable thermodynamic effect of cavitation. From these experimental data, the cavitation performance for a given pump can be predicted for any liquid, liquid temperature, and rotative speed provided that flow similarity (constant ψ/ψ_{NC} and ϕ) is maintained. However, for the present study, only changes in liquid temperature at specified values of flow coefficient ϕ are considered.

The required NPSH values at nominal temperatures of 27.9° and 30.9° R (15.5° and 17.2° K) from figure 6 were used in equation 4 to obtain a value for $\Delta h_{v_2} - \Delta h_{v_1}$ at a given flow coefficient. An assumed value of Δh_{v_1} was used in an iterative process with figure 7 (eq. (1)) and equation (3) to solve for values of Δh_{v_1} and Δh_{v_2} that satisfy equation (4). The thermodynamic effect of cavitation at other temperatures were then predicted using equation (3) and a reference value of vapor to liquid volume ratio obtained from the determined value of Δh_{v_1} .

The predicted magnitude of the thermodynamic effect of cavitation is shown in figure 8 as a function of flow coefficient for a range of liquid hydrogen temperatures. Since the thermodynamic effect of cavitation is zero at the hydrogen triple point temperature of 24.9° R (13.8° K), the predicted curve would be the abscissa of figure 8. A value of Δh_v taken from figure 8 represents the predicted absolute value of thermodynamic effect of cavitation with respect to the condition where the thermodynamic effect is zero ($\Delta h_v = 0$). These trends in thermodynamic effects of cavitation for this inducer will be discussed later.

A comparison between experimental and predicted values of required NPSH for this inducer at a 0.70 head coefficient ratio is shown in figure 9. The data points are repeated from figure 6, as are reference data (solid lines) at 27.9° and 30.9° R (15.5° and 17.2° K) which were used to predict the required NPSH at other temperatures. The predicted values are shown as dashed lines. The liquid hydrogen data at 32° and 34° R (17.8° and 18.9° K) compare reasonably well with the predicted curves at values of

NPSH above the inlet line vapor region. Values of NPSH less than the calculated velocity head $v_a^2/2g$ are again indicated by the shaded area.

The change in required NPSH with hydrogen temperature is quite significant as shown in figure 9. At a given flow coefficient, the change in required NPSH for constant increments of temperature becomes smaller as the hydrogen temperature approaches the triple point. This change in required NPSH is due to a decrease in the thermodynamic effects of cavitation at the lower temperatures (fig. 8). The reduction in thermodynamic effects is primarily caused by the decrease in the slope of the vapor pressure-temperature curve and by the lower vapor density as the hydrogen temperature approaches the triple point.

The data of figure 9 also show that, as the flow coefficient is decreased, the required NPSH curves for any two given temperatures diverge. This indicates as do the curves of figure 8 that the thermodynamic effects of cavitation for this inducer increase as the flow coefficient is decreased. For example, at a flow coefficient of 0.076 in figure 8 for a temperature of 34°R (18.9°K), the predicted thermodynamic effect of cavitation is 40 feet (12.2 m), while at a lower flow coefficient of 0.060 for the same temperature the magnitude increases to 72 feet (21.9 m). This increase in magnitude may result from the sharper pressure distribution on the blade suction surface as the angle of fluid incidence increases at the lower flow coefficient. This trend with flow coefficient is in agreement with results of reference 14 in which the influence of pressure distribution on the thermodynamic effect of cavitation was studied. The venturi cavitation studies of reference 14 show that the largest reduction in vapor pressure occurred with a venturi contour which had the sharpest pressure distribution.

The required NPSH for a given flow coefficient and hydrogen temperature can be adjusted to the NPSH that would be required in triple point hydrogen where the thermodynamic effect of cavitation would be zero. For each data point shown in figure 6, the magnitude of the thermodynamic effect of cavitation at the corresponding temperature and flow coefficient can be determined from figure 8. This value of Δh_v , (thermodynamic effect of cavitation) when added to the measured required NPSH as obtained from figure 6, yields the required NPSH for a fluid which exhibits no thermodynamic effect of cavitation (eq. (4)). The NPSH data of figure 6 were adjusted to this condition of zero thermodynamic effect of cavitation and the results are shown in figure 10. The dashed line in figure 10, which represents the estimated hydrogen performance at the triple point temperature (from fig. 9), is in reasonably good agreement with the adjusted NPSH data. This agreement suggests that the semiempirical method of reference 4 may be useful in generalizing experimental NPSH data when only minimum data are available. For example, in a fluid that exhibits thermodynamic effects of cavitation, data taken at various liquid temperatures can be adjusted to any convenient temperature. Similarly as

shown in reference 4 data at different pump speeds can be normalized to a desired speed by use of the semiempirical prediction method.

An inducer identical to the one reported herein was operated in room temperature water at 10 000 rpm to obtain data for comparison with the hydrogen results. To allow comparison of the water and hydrogen data on the same basis, the estimated triple point hydrogen curve from figure 10 was normalized to 10 000 rpm by the ratio of the square of the rotational speeds. These normalized hydrogen results are compared with the room temperature water data in figure 11 where the required NPSH for each liquid is shown as a function of flow coefficient for a 0.70 head coefficient ratio. The agreement between the hydrogen and water data shows that the triple point hydrogen curve approximates the NPSH requirement in room temperature water where the thermodynamic effect of cavitation is essentially zero.

In reference 3, an investigation of a similar 84° helical inducer (different leading edge fairing) was made in room temperature water and 37° R (20.6° K) liquid hydrogen. The required NPSH in 37° R (20.6° K) liquid hydrogen was reported to be 90 feet (27.4 m) less than that required in room temperature water at a flow coefficient of 0.076. The predicted magnitude of the thermodynamic effect of cavitation from figure 8 is 87 feet (26.6 m) at comparable operating conditions. Thus there is good agreement between the predicted value and the experimentally determined value of reference 3.

SUMMARY OF RESULTS

The net positive suction head NPSH requirement for an 84° constant lead axial flow inducer was evaluated over a range of flow coefficient from 0.060 to 0.074 in low temperature liquid hydrogen at a rotative speed of 20 000 rpm. The range of liquid hydrogen temperature studied was from 27.9° to 36.6° R (27.9° to 17.2° K). An available semiempirical method was used to predict the magnitude of the thermodynamic effect of cavitation for various flow coefficients and hydrogen temperatures. A comparison between experimental and predicted values of required net positive suction head was made at a head coefficient ratio of 0.70. The principal results of this investigation are the following:

1. As the hydrogen inlet temperature was lowered, higher values of NPSH were required to maintain the same inducer performance level because of a decrease in the thermodynamic effect of cavitation at the lower temperature. The thermodynamic effect of cavitation becomes negligible as the hydrogen temperature approaches its triple point temperature.
2. The magnitude of the thermodynamic effect of cavitation increased substantially as the flow coefficient was decreased. For this inducer at a hydrogen temperature of

34° R (18.9° K) the predicted magnitude of the thermodynamic effect of cavitation increased from 40 feet (12.2 m) at a flow coefficient of 0.076 to 72 feet (21.9 m) at a flow coefficient of 0.060.

3. Reasonable agreement was obtained between predicted and experimentally determined values of required NPSH over the range of flow coefficient and liquid hydrogen temperature.

4. Using a semiempirical prediction method, the required NPSH at several hydrogen temperatures was adjusted to the required NPSH in hydrogen at the triple point temperature (zero thermodynamic effect of cavitation). Good agreement was obtained when the normalized triple point hydrogen curve was compared with data for an identical inducer operated in room temperature water.

Lewis Research Center,
National Aeronautics and Space Administration,
Cleveland, Ohio, November 8, 1967,
128-31-02-24-22.

APPENDIX - SYMBOLS

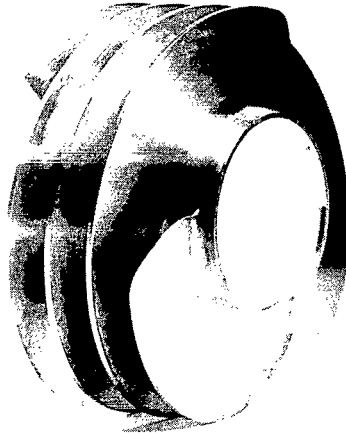
C_p	specific heat of liquid, Btu/(lb _m)(°R) or J/(kg)(°K)
dH_{vp}/dT	slope of vapor pressure head to temperature curve, ft/°R (m/°K)
g	acceleration due to gravity, ft/sec ² (m/sec ²)
ΔH	pump head rise based on inlet density, ft (m) of liquid
Δh_v	decrease in vapor pressure because of vaporization (magnitude of thermodynamic effect of cavitation), ft (m) of liquid
k	liquid thermal conductivity, Btu/(hr)(ft)(°R) or J/(hr)(m)(°K)
L	latent heat of vaporization, Btu/lb _m (J/kg)
N	rotative speed, rpm
$NPSH$	net positive suction head, ft (m) of liquid
U_t	blade tip speed, ft/sec (m/sec)
V_a	average axial velocity at inducer inlet, ft/sec (m/sec)
V_l	volume of liquid involved in cavitation process, cu in. (cc)
V_o	free stream velocity, ft/sec (m/sec)
V_v	volume of vapor, cu in. (cc)
Δx	length of cavity, in. (cm)
α	thermal diffusivity of liquid, $k/\rho_l C_p$, sq ft/hr, (sq m/hr)
ρ_l	density of liquid, lb _m /cu ft (kg/cm ³)
ρ_v	density of vapor, lb _m /cu ft (kg/cm ³)
ϕ	flow coefficient, V_a/U_t
ψ	head coefficient, $g \Delta H/U_t^2$
Subscripts:	
a	adjusted
NC	noncavitating
ref	reference value obtained from experimental tests
$1, 2$	given test condition

REFERENCES

1. Carney, R. R.: "Slush Hydrogen" Production and Handling as a Fuel for Space Projects. *Advances in Cryogenic Engineering*. Vol. 9. K. D. Timmerhaus, ed., Plenum Press, 1964, pp. 529-536.
2. Mann, D. B.; Ludtke, P. R.; Sindt, C. F.; and Chelton D. B.: *Liquid-Solid Mixtures of Hydrogen near the Triple Point*. *Advances in Cryogenic Engineering*. Vol. 11. K. D. Timmerhaus, ed., Plenum Press, 1966, pp. 207-217.
3. Ball, Calvin L.; Meng, Phillip R.; and Reid, Lonnie: *Cavitation Performance of 84° Helical Pump Inducer Operated in 37° and 42° R Liquid Hydrogen*. NASA TM X-1360, 1967.
4. Ruggeri, Robert S.; Moore, Royce D.; and Gelder, Thomas F.: *Method for Predicting Pump Cavitation Performance*. Paper presented at the Ninth Liquid Propulsion Symposium, Interagency Chemical Rocket Propulsion Group, St. Louis, Oct. 25-27, 1967.
5. Wilcox, Ward W.; Meng, Phillip R.; and Davis, Roger L.: *Performance of an Inducer-Impeller Combination at or near Boiling Conditions for Liquid Hydrogen*. *Advances in Cryogenic Engineering*. Vol. 8. K. D. Timmerhaus, ed., Plenum Press, 1963, pp. 446-455.
6. Gelder, Thomas F.; Ruggeri, Robert S.; and Moore, Royce D.: *Cavitation Similarity Considerations Based on Measured Pressure and Temperature Depressions in Cavitated Regions of Freon 114*. NASA TN D-3509, 1966.
7. Ruggeri, Robert S.; and Gelder, Thomas F.: *Cavitation and Effective Liquid Tension of Nitrogen in a Tunnel Venturi*. NASA TN D-2088, 1964.
8. Salemann, Victor: *Cavitation and NPSH Requirements of Various Liquids*. *J. Basic Eng.*, vol. 81, no. 2, June 1959, pp. 167-180.
9. Spraker, W. A.: *The Effects of Fluid Properties on Cavitation in Centrifugal Pumps*. *J. Eng. Power*, vol. 87, no. 3, July 1965, pp. 309-318.
10. Stepanoff, A. J.: *Cavitation Properties of Liquids*. *J. Eng. Power*, vol. 86, no. 2, Apr. 1964, pp. 195-200.
11. Jacobs, Robert B.: *Prediction of Symptoms of Cavitation*. *J. Res. Natl. Bur. Std., Eng and Instrumentation*, vol. 65, no. 3, July-Sept. 1961, pp. 147-156.
12. Meng, Phillip R.; and Connelly, Robert E.: *Investigation of Effects of Simulated Nuclear Radiation Heating on Inducer Performance in Liquid Hydrogen*. NASA TM X-1359, 1967.

13. Pinkel, I. I.; Hartmann, M. J.; Hauser, C. H.; Miller, M. J.; Ruggeri, R. S.; and Soltis, R. F.: Pump Technology. Selected Technology for the Petroleum Industry. NASA SP-5053, 1966, pp. 81-101.
14. Moore, Royce D.; Ruggeri, Robert S.; and Gelder, Thomas F.: Effects of Wall Pressure Distribution and Liquid Temperature on Incipient Cavitation of Freon-114 and Water in Venturi Flow. NASA TN D-4340, 1967.

Helix angle (at tip), deg	84
Rotor tip diameter, in. (cm)	4.986 (12.664)
Rotor hub diameter, in. (cm)	2.478 (6.294)
Hub-tip ratio	0.497
Number of blades	3
Axial length, in. (cm)	2.00 (5.08)
Peripheral extent of blades, deg	440
Tip chord length, in. (cm)	19.14 (48.62)
Hub chord length, in. (cm)	9.51 (24.16)
Solidity	3.838
Tip blade thickness, in. (cm)	0.067 (0.170)
Hub blade thickness, in. (cm)	0.100 (0.254)
Calculated radial tip clearance (at hydrogen temperature), in. (cm)	0.025 (0.064)
Ratio of tip clearance to blade height	0.020
Material	6061-T6 aluminum



C-67-423

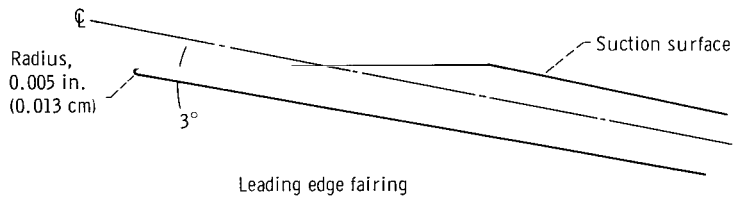


Figure 1. - Photograph and geometric details of 84° inducer.

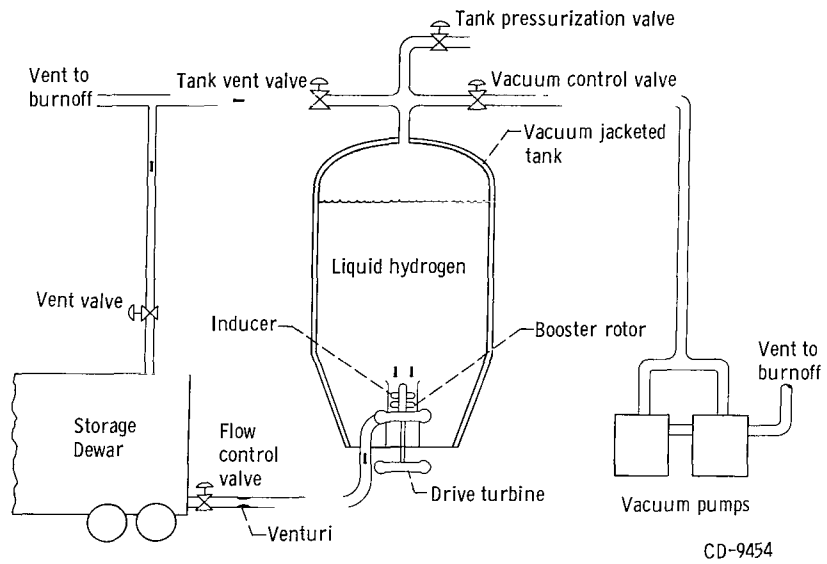
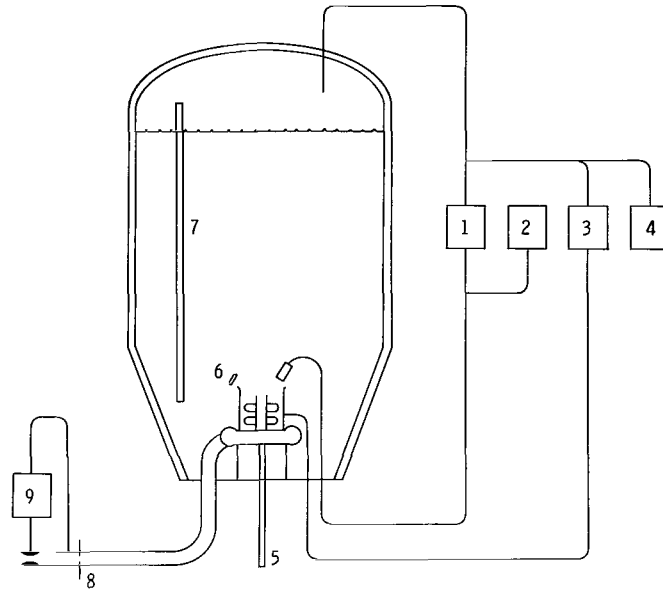


Figure 2. - Schematic view of liquid hydrogen pump test facility.



Item number	Parameter	Estimated system accuracy	Number used	Remarks
1	Net positive suction head, NPSH	± 0.05 psi (0.35 newton/cm ²)	1	Measured as differential pressure (converted to head of liquid) between vapor bulb at pump inlet and tank pressure corrected to pump inlet conditions
2	Vapor pressure	± 0.25 psi (1.7 newton/cm ²)	1	Vapor bulb charged with liquid hydrogen from research tank
3	Inducer pressure rise	± 0.5 psi (3.5 newton/cm ²)	1	Shielded total pressure rake at mid-passage 1 inch (2.54 cm) downstream of inducer
4	Tank pressure	± 1.0 psi (6.9 newton/cm ²)	1	Measured in tank ullage and corrected to pump inlet conditions for use as reference pressure for differential transducers
5	Rotative speed	± 100 rpm	1	Magnetic pickup in conjunction with gear on turbine drive shaft
6	Pump inlet temperature	$\pm 0.1^\circ$ R (0.06° K)	2	Platinum resistor probes 180° apart at inlet
7	Liquid level	± 0.5 ft (0.15 m)	1	Capacitance gage, used for hydrostatic head correction to pump inlet conditions
8	Venturi inlet temperature	$\pm 0.1^\circ$ R (0.06° K)	2	Platinum resistor probes 180° apart upstream of Venturi
9	Venturi differential pressure	± 0.10 psi (0.7 newton/cm ²)	1	Venturi calibrated in air and water

Figure 3. - Instrumentation for liquid hydrogen pump test facility.

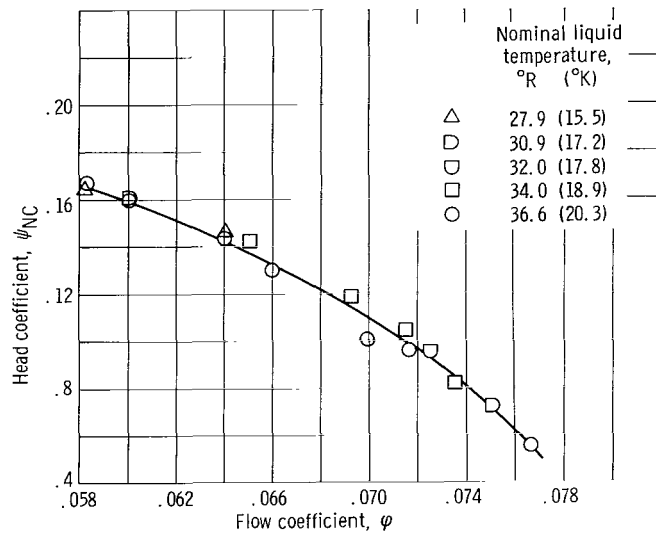
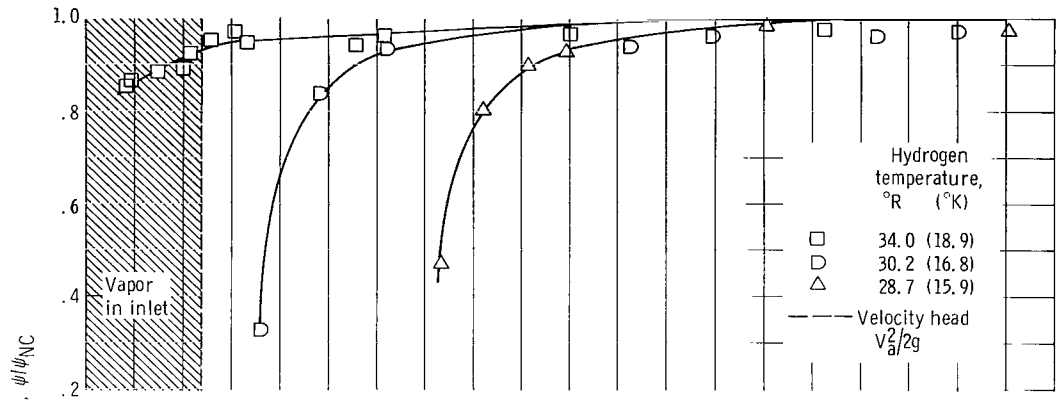
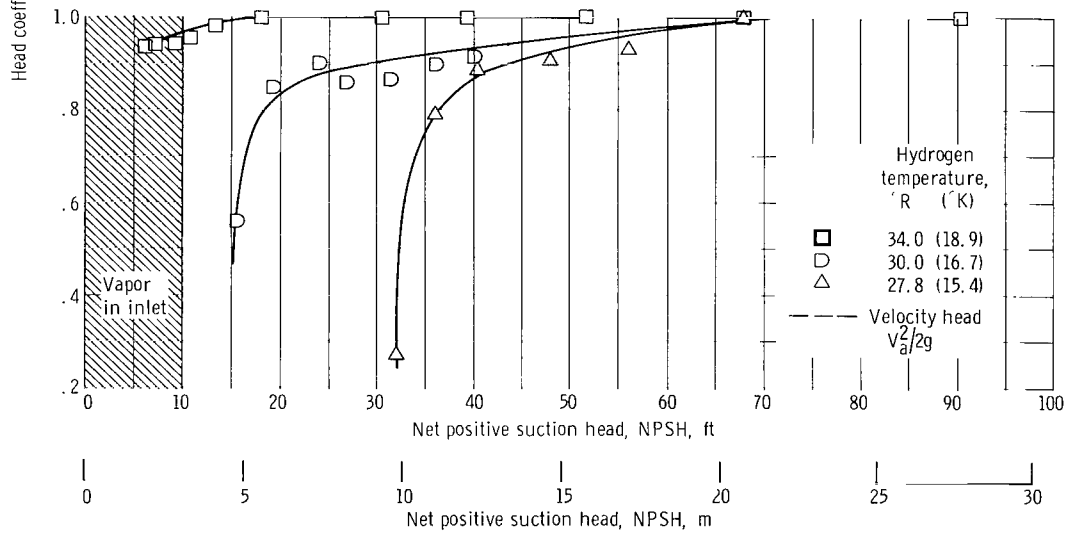


Figure 4. - Noncavitating performance of 84° inducer in hydrogen at rotative speed of 20 000 rpm. Net positive suction head, 170 feet (51.8 m).

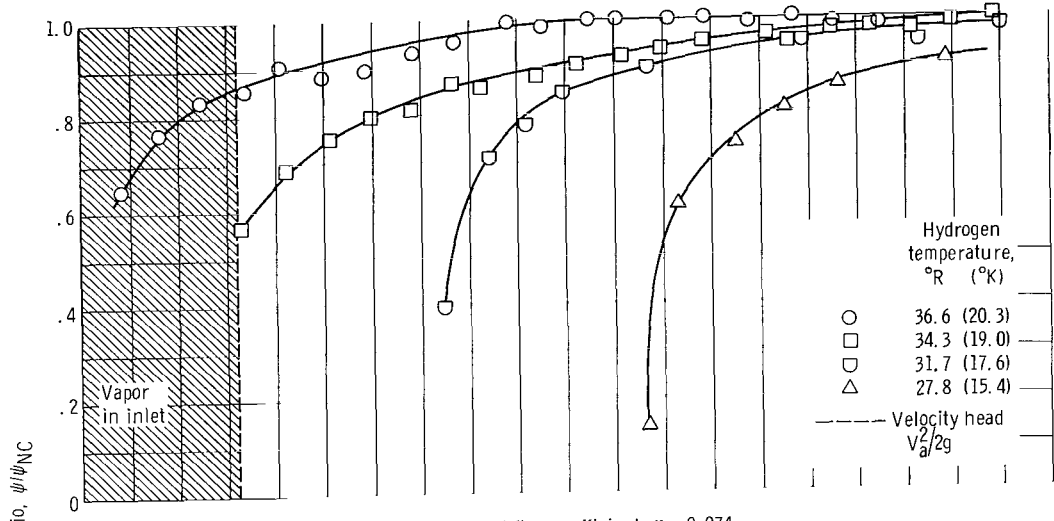


(c) Nominal flow coefficient $\varphi = 0.065$.

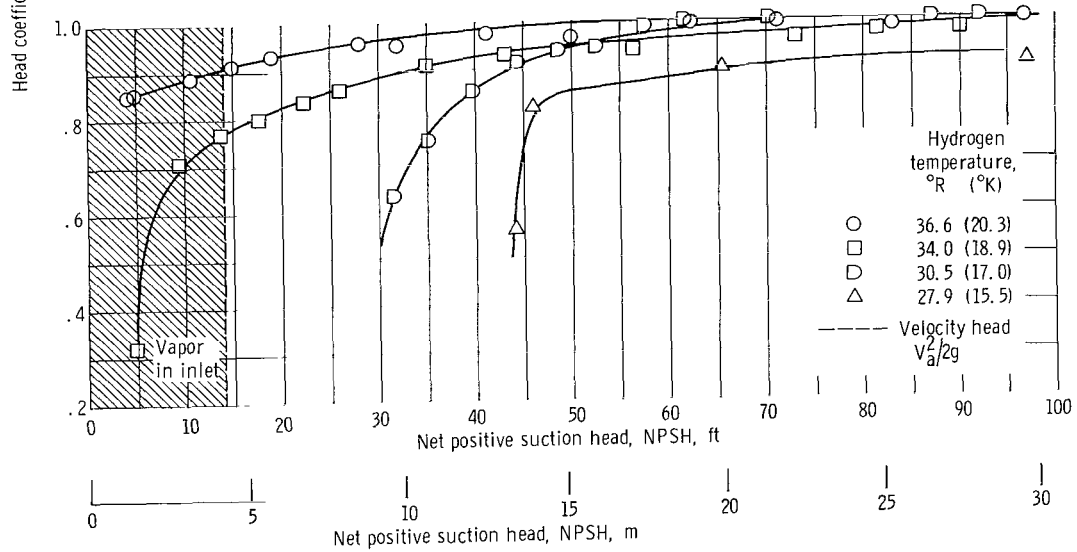


(d) Nominal flow coefficient $\varphi = 0.060$.

Figure 5. - Concluded.



(a) Nominal flow coefficient $\phi = 0.074$.



(b) Nominal flow coefficient $\phi = 0.070$.

Figure 5. - Cavitation performance of 84° inducer in hydrogen at 20 000 rpm.

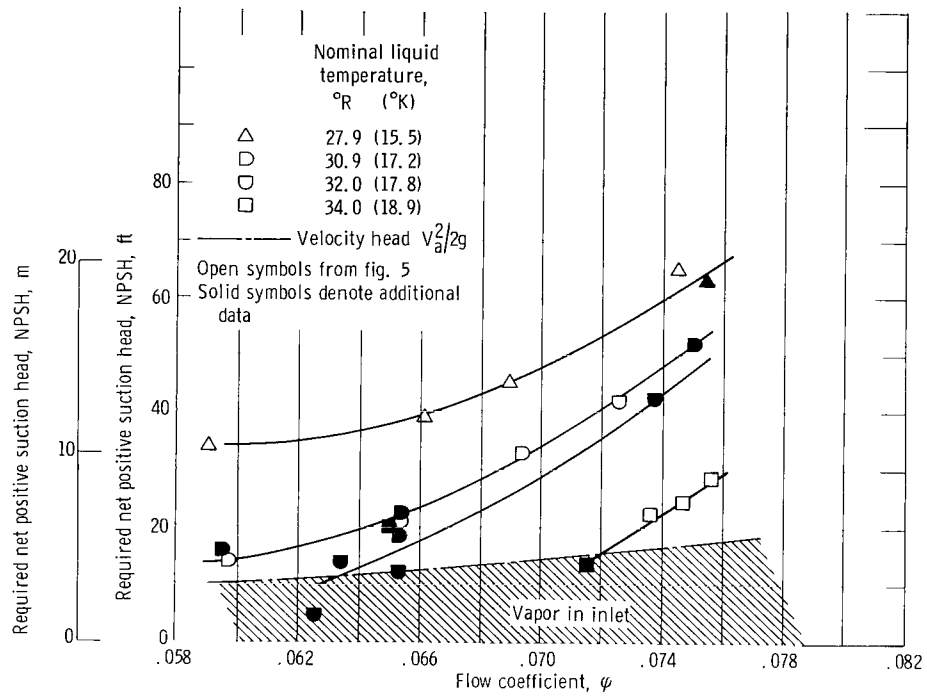


Figure 6. - Variation of inducer cavitation performance with flow coefficient at several hydrogen temperatures. Rotative speed, 20 000 rpm; head coefficient ratio, 0.70.

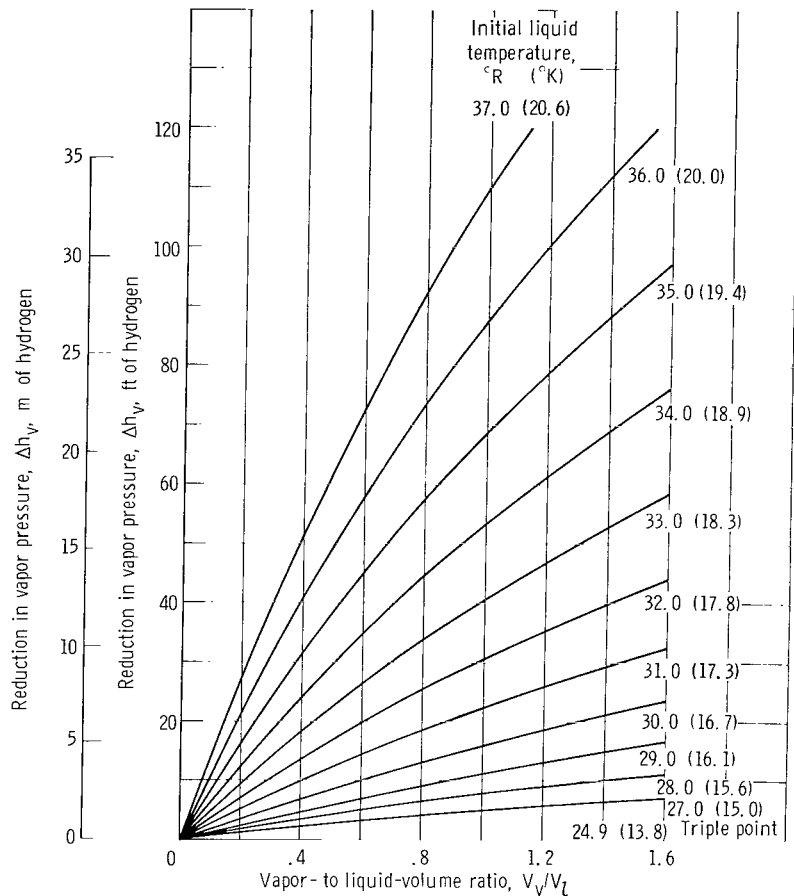


Figure 7. - Calculated vapor pressure reduction due to vaporization as function of volume ratio for several liquid hydrogen temperatures.

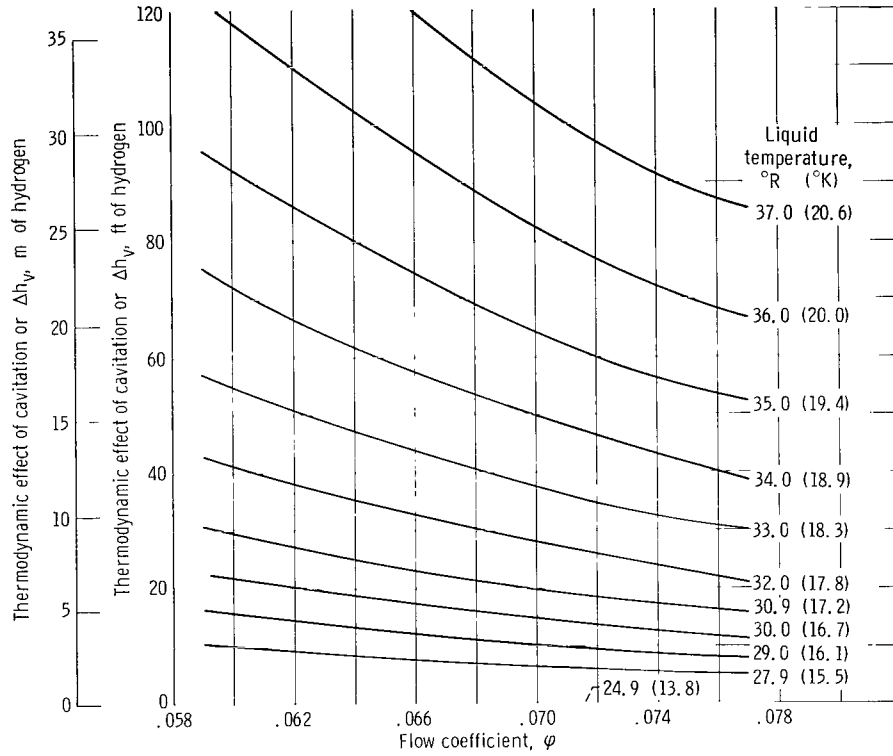


Figure 8. - Predicted thermodynamic effects of cavitation as function of flow coefficient for several liquid hydrogen temperatures for 84° inducer. Rotative speed, 20 000 rpm; head coefficient ratio, 0.70.

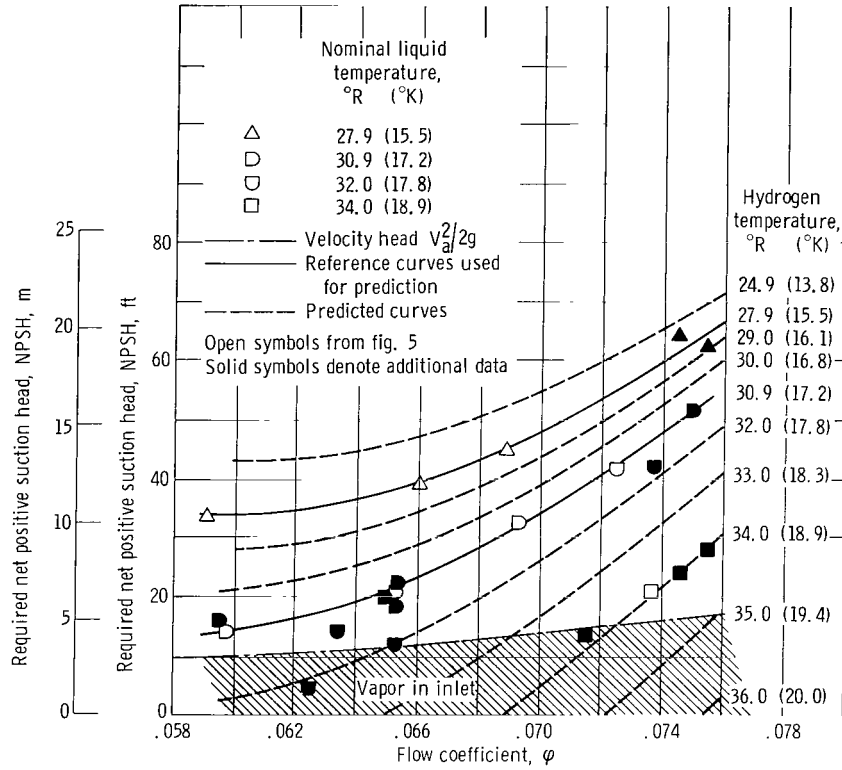


Figure 9. - Comparison of predicted and measured required net positive suction head for 84° inducer in hydrogen. Rotative speed, 20 000 rpm; head coefficient ratio, 0.70.

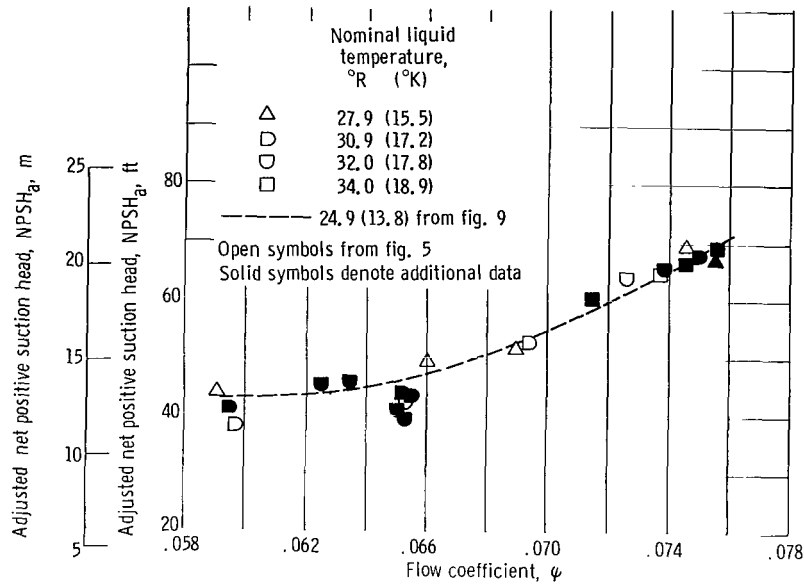


Figure 10. - Required net positive suction head for 84° inducer in hydrogen adjusted to performance at hydrogen triple point temperature. Rotative speed, 20 000 rpm; head coefficient ratio, 0.70.

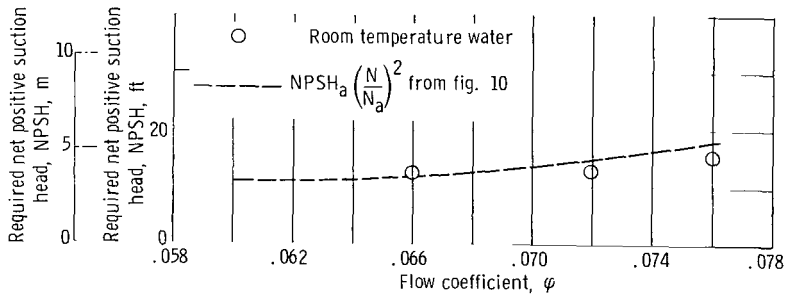


Figure 11. - Comparison of required net positive suction head in triple point temperature hydrogen and room temperature water for 84° inducer. Rotative speed, 10 000 rpm; head coefficient ratio, 0.70.

02U 001 53 51 3DS 68059 00903
AIR FORCE WEAPONS LABORATORY/AFWL/
KIRTLAND AIR FORCE BASE, NEW MEXICO 87117

ATTN: MISS MADELINE F. CANOVA, CHIEF TECHNICAL
LIBRARY /WTLI/

POSTMASTER: If Undeliverable (Section 158
Postal Manual) Do Not Return

"The aeronautical and space activities of the United States shall be conducted so as to contribute . . . to the expansion of human knowledge of phenomena in the atmosphere and space. The Administration shall provide for the widest practicable and appropriate dissemination of information concerning its activities and the results thereof."

—NATIONAL AERONAUTICS AND SPACE ACT OF 1958

NASA SCIENTIFIC AND TECHNICAL PUBLICATIONS

TECHNICAL REPORTS: Scientific and technical information considered important, complete, and a lasting contribution to existing knowledge.

TECHNICAL NOTES: Information less broad in scope but nevertheless of importance as a contribution to existing knowledge.

TECHNICAL MEMORANDUMS: Information receiving limited distribution because of preliminary data, security classification, or other reasons.

CONTRACTOR REPORTS: Scientific and technical information generated under a NASA contract or grant and considered an important contribution to existing knowledge.

TECHNICAL TRANSLATIONS: Information published in a foreign language considered to merit NASA distribution in English.

SPECIAL PUBLICATIONS: Information derived from or of value to NASA activities. Publications include conference proceedings, monographs, data compilations, handbooks, sourcebooks, and special bibliographies.

TECHNOLOGY UTILIZATION PUBLICATIONS: Information on technology used by NASA that may be of particular interest in commercial and other non-aerospace applications. Publications include Tech Briefs, Technology Utilization Reports and Notes, and Technology Surveys.

Details on the availability of these publications may be obtained from:

SCIENTIFIC AND TECHNICAL INFORMATION DIVISION
NATIONAL AERONAUTICS AND SPACE ADMINISTRATION

Washington, D.C. 20546